

Recurrence Time Statistics for Chaotic Systems and Their Applications

J. B. Gao

Department of Electrical Engineering, University of California at Los Angeles, Los Angeles, California 90095
(Received 5 April 1999)

By studying recurrence time statistics for chaotic systems, we identify two different types of recurrences and develop scaling laws relating the mean recurrence time to the information dimension of the chaotic attractor. We then design two novel and simple ways of using the recurrence time statistics for analyzing transient as well as nonstationary time series. We show that the methods are capable of detecting nonstationarity due to drift of parameters, locating bifurcations, telling the periodicity of major transient periodic motions, and other types of changes in the dynamics.

PACS numbers: 05.45.Tp, 02.50.Fz

Since the time of Boltzmann and Poincaré, the study of the recurrence of states of a dynamical system (i.e., how often a small region in phase space is visited) has been recognized to be fundamental to classical statistical mechanics [1]. It is also of central importance in the study of chaos [2]. However, recurrence time statistics for chaotic systems has only been considered for 1D discrete maps [3] and for a model stationary flow [4]. Thus, an important and challenging question is whether a scaling law relating the mean recurrence time to the attractor dimensions and/or Lyapunov exponents can be developed for multivariate chaotic systems.

Almost all existing linear and nonlinear time series analysis techniques assume that the time series is stationary. However, many time series occurring in geophysics, physiology, finance, etc., are nonstationary. Sometimes the changes in the dynamics can be the most interesting feature of a phenomenon under study. Thus, simple and efficient methods capable of detecting the nonstationarity of a time series and studying transient dynamics would be valuable to researchers from diverse fields. This subject has attracted much attention recently [5–10]. In this Letter, we first consider the recurrence time statistics for multivariate chaotic systems. We shall identify recurrence times of two different types and derive scaling laws relating the mean recurrence times of these two types to the information dimension of the attractor. We then design two simple and novel algorithms that use the recurrence time statistics for analyzing transient as well as nonstationary dynamics.

Given a chaotic dynamical system described either by a discrete map or by a set of ordinary differential equations (ODEs), we first iterate the map or integrate the ODEs (with sampling time τ) until the dynamics is free of transience. We then arbitrarily choose a reference point X_0 on the attractor and consider recurrence to its neighborhood of radius r : $B_r(X_0) = \{X : \|X - X_0\| \leq r\}$. If the underlying dynamics on the chaotic attractor is ergodic, then X_0 can be chosen arbitrarily. Next, we consider a trajectory of length N and denote the subset of the trajectory that belongs to $B_r(X_0)$ by $S_1 = \{X_{t_1}, X_{t_2}, \dots, X_{t_i}, \dots\}$. These are the Poincaré recurrence points, and the Poincaré re-

currence times are simply defined as $\{T_1(i) = t_{i+1} - t_i, i = 1, 2, \dots\}$. For later convenience, we call $\{T_1(i)\}$ the recurrence times of the first type.

Sometimes we may have $T_1(i) = \tau$ (τ being 1 for maps), for some i . This corresponds to both X_{t_i} and $X_{t_i+\tau}$ belonging to S_1 . For continuous time systems with fixed (small) τ , if the radius r of $B_r(X_0)$ is not too small, we can have a sequence such as $X_{t_i}, X_{t_i+\tau}, \dots, X_{t_i+k\tau}$ belonging to S_1 , with k on the order of 10 or even larger. This is schematically shown in Fig. 1. We call the sequence $X_{t_i+\tau}, \dots, X_{t_i+k\tau}$ (excluding X_{t_i}) sojourn points. When k is on the order of 10, each such sequence of points effectively represents a 1D set. For maps or continuous time systems with small r , sojourn points are negligible and form a 0D (empty or almost empty) set. Now we remove these points from S_1 and denote the remaining points of S_1 by $S_2 = \{X_{t'_1}, X_{t'_2}, \dots, X_{t'_i}, \dots\}$, which defines a time sequence $\{T_2(i) = t'_{i+1} - t'_i, i = 1, 2, \dots\}$. We call S_2 the recurrence points of the second type and $T_2(i)$ the recurrence times of the second type.

We now develop scaling laws for the mean recurrence times of these two types, $\bar{T}_1(r)$ and $\bar{T}_2(r)$. Recall that the pointwise dimension d_p is defined [11] by $\mu(B_r(X_0)) \sim r^{d_p}$, where $\mu(B_r(X_0))$ is the measure associated with $B_r(X_0)$. Since $\mu(B_r(X_0)) = \mu(S_1)$, while $\mu(S_1)$ can be estimated by how frequently $B_r(X_0)$ is visited by a

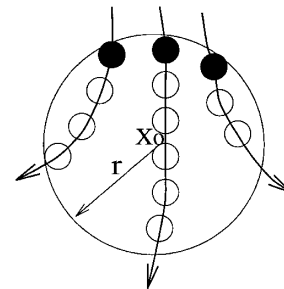


FIG. 1. A schematic showing the recurrence points of the second type (solid circles) and the sojourn points (open circles) in $B_r(X_0)$.

trajectory, we thus have $\mu(S_1) = \frac{N/(\bar{T}_1(r)/\tau)}{N}$ and

$$\bar{T}_1(r) \sim r^{-d_p}. \quad (1)$$

The quantity $\bar{T}_1(r)/r^{-d_p}$ typically depends on the reference point X_0 . This reflects the fact that some part of the attractor will be visited more frequently than other parts. Since d_p and the information dimension d_1 typically have a common value [11], we can substitute d_p by d_1 in Eq. (1).

Similarly, we have $\mu(S_2) \sim \bar{T}_2(r)^{-1}$. When the sojourn points represent a 0D set, $\mu(S_2) = \mu(S_1) \sim r^{d_1}$. When the sojourn points represent a 1D set, $\mu(S_2) \sim r^{d_1-1}$. Hence, for discrete maps and for continuous time systems with small r ,

$$\bar{T}_2(r) \sim r^{-d_1}, \quad (2)$$

and for continuous time systems with large r ,

$$\bar{T}_2(r) \sim r^{-(d_1-1)}. \quad (3)$$

To verify the above scaling laws, consider the entire system of the Henon map [12],

$$\begin{aligned} x(n+1) &= 1 + y(n) - 1.4x(n)^2, \\ y(n+1) &= 0.3x(n). \end{aligned} \quad (4)$$

and the chaotic Lorenz attractor [13],

$$\begin{aligned} dx/dt &= -10(x - y), & dy/dt &= -xz + 28x - y, \\ dz/dt &= xy - 8z/3. \end{aligned} \quad (5)$$

The Lorenz system was integrated using a fourth-order Runge-Kutta method with sampling time $\tau = 0.001$. For each system, we arbitrarily select a point on the attractor as a reference point X_0 and then compute $\bar{T}_1(r)$ and $\bar{T}_2(r)$ recurring to $B_r(X_0)$. Figure 2 shows the variations of $\bar{T}_1(r)$ (circles) and $\bar{T}_2(r)$ (squares) with r (in logarithmic

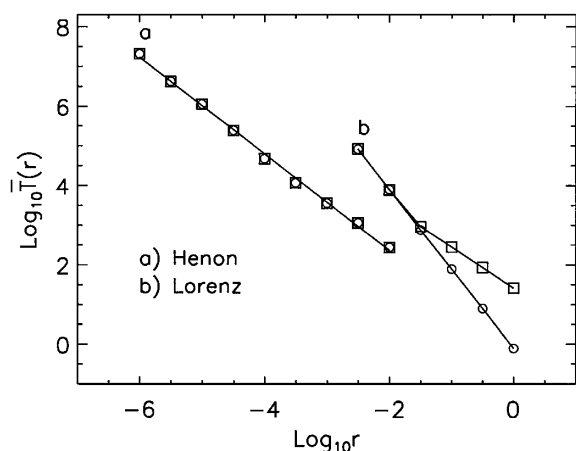


FIG. 2. Variations of $\bar{T}_1(r)$ (denoted by circles) and $\bar{T}_2(r)$ (denoted by squares) with r (in logarithmic scale) for (a) the Henon map and (b) the Lorenz system.

scale) for the two systems. We observe clearly that, for the Henon map, $\bar{T}_1(r)$ and $\bar{T}_2(r)$ are the same, and they follow the scaling laws of Eqs. (1) and (2). For the Lorenz system, $\bar{T}_1(r)$ and $\bar{T}_2(r)$ are also the same at small r and also follow the scaling laws of Eqs. (1) and (2). At large r , $\bar{T}_2(r)$ follows the scaling law described by Eq. (3). The slopes estimated from these lines are $d_1 = 1.24$ for the Henon map, and $d_1 = 2.03$ and $d_1 - 1 = 1.02$ for the Lorenz system. These values for the information dimensions of these two systems are consistent with the results of [14]. We note that the validity of Eqs. (1)–(3) was also tested and verified using the chaotic Rossler system.

Equations (1)–(3) imply that, if a system has a very large number of degrees of freedom (i.e., d_1 is large) and r is small, the mean recurrence time is prohibitively long. This is typically true for systems treated in classical statistical mechanics [1]. Even if a system is low dimensional, we still need to decide how many recurrences are needed to reliably estimate $\bar{T}_1(r)$ and $\bar{T}_2(r)$ for each r . Were $\bar{T}_1(r)$ and $\bar{T}_2(r)$ to follow a power law distribution, as is the case in a 1D chaotic map containing a marginally stable fixed point [3] or in anomalous diffusion [4], then a very large number of recurrences are needed to calculate $\bar{T}_1(r)$ and $\bar{T}_2(r)$. Hence we need to consider the distributions for $T_1(r)$ and $T_2(r)$. It turns out that the distribution for $T_1(r)$ is difficult to work with, due to the coexistence of a deterministic part (the sojourn times), and a random part (the recurrence times of the second type). The distribution for $T_2(r)$ is, however, very simple. In order for a trajectory to return to $B_r(X_0)$ (with r small) after leaving it, folding on the attractor has to have occurred at least once. This means that the information on the exact locations of the earlier recurrence points of the second type is no longer helpful in predicting when and where future recurrences will occur. In other words, when a recurrence occurs, the system has no memory as to when and where the last recurrence occurred. This means $T_2(i)$ ought to be longer than the prediction time scale. The latter is given by $1/\lambda_{\max}$, with λ_{\max} being the largest positive Lyapunov exponent. These arguments can be simply expressed by the following inequality:

$$\bar{T}_2(r) > 1/\lambda_{\max}. \quad (6)$$

The memoryless property of $T_2(i)$ also suggests that $T_2(i)$ follows an exponential distribution, as Fig. 3 shows for the Henon map and the Lorenz system. That $T_2(i)$ follows an exponential distribution is quite beneficial to us, as the standard deviation of an exponentially distributed random variable equals its mean. Thus, if we estimate $\bar{T}_2(r)$ by the sample mean of K observations $\{T_2(r)\}$, then the error bar for $\bar{T}_2(r)$ is $\bar{T}_2(r)/\sqrt{K}$.

Next we develop two simple algorithms for the analysis of transient as well as nonstationary dynamics. From now on, we shall focus on the analysis of scalar time series so that the methods developed here can be directly applied

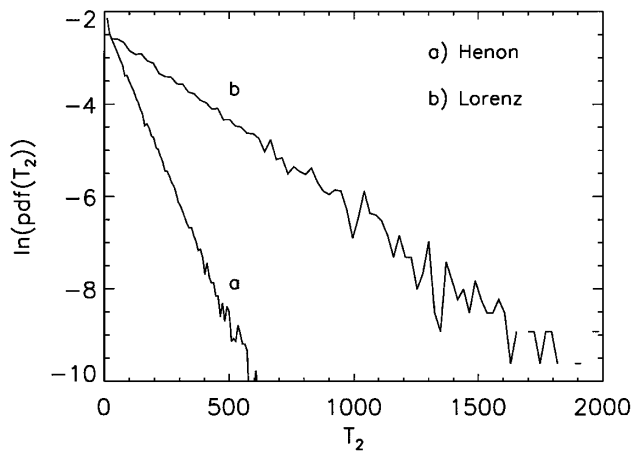


FIG. 3. Probability density function (pdf) for $\{T_2(r)\}$ for (a) the Henon map and (b) the Lorenz system. The scale r is 10^{-3} and 10^{-2} for (a) and (b), respectively.

to the analysis of experimental data. Using a time delay embedding technique [15], we construct vectors of the form, $X_i = [x(i), x(i+L), \dots, x(i+(m-1)L)]$, with $\{x(i), i=1, 2, \dots\}$ being a scalar time series, m being the embedding dimension, and L being the delay time. We shall analyze the behavior of $\bar{T}_2(r)$ to develop our algorithms. $\bar{T}_1(r)$ also contains useful information about the changes in the dynamics due to the presence of transience or nonstationarity. Because the number of sojourn points depends upon phase velocity, $\bar{T}_1(r)$ is sensitively dependent on embedding parameters. Analysis and interpretation are therefore more difficult.

The design of our methods is based on the observation that, due to nonstationarity, successive recurrence times will, on average, be changing with time. In our first algorithm, we first partition a long time series into (overlapping or nonoverlapping) blocks of data sets of short length. We then compute $\bar{T}_2(r)$ for each subdata set. For nonstationary and transient time series, we expect to observe that $\bar{T}_2(r)$ will be different for different blocks of subdata sets. In our second algorithm, we compute $T_2(j)$ for different reference points from the whole data set, where j denotes j th return to the reference point. Nonstationarity is reflected through the variation of $T_2(j)$ with j . We shall detail these methods by studying the transient logistic map [6] and the generalized Baker's map [10].

We employ our first algorithm to study the transient dynamics of the logistic map: $x_{n+1} = ax_n(1-x_n)$. Following Trulla *et al.* [6], we first generate a transient time series consisting of 120 001 points, x , by consistently incrementing parameter a in steps of 0.00001 on each iteration. We then compute $\bar{T}_2(r)$ on time series data within episodic windows consisting of 800 consecutive points. Sequential windows are shifted by 10 points (thus overlapping by 790 points), giving a total of 11 920 values for $\bar{T}_2(r)$. We also follow Trulla *et al.* [6] by choosing $m=2$ and $L=1$. Figure 4 shows the variation of $\bar{T}_2(r)$ with the parameter

a . The scale r is chosen to be 2^{-5} . We have observed that, as long as r is not too large, the $\bar{T}_2(r)$ vs a curve does not change much with r . We observe from Fig. 4 that the behavior of $\bar{T}_2(r)$ with a not only correctly locates the bifurcations but also correctly indicates the periodicity of the major transient periodic motions, such as periods 2 and 4 in the main period-doubling cascade, and period 3 in the period(3)-doubling cascade. This is as expected, since $\bar{T}_2(r)$ simply estimates the periodicity for periodic motions. We also observe that there are four large dips (in addition to the bifurcations) in the $\bar{T}_2(r)$ vs a curve, which are right above the letters A, B, C, and D. These dips correspond to the small dips in the Lyapunov exponent vs the bifurcation parameter curve computed by Trulla *et al.* [6] using the transient time series. The small dips in that curve of [6] become larger when the Lyapunov exponent is computed in a finer resolution [16]. This indicates that $\bar{T}_2(r)$ can also effectively pick up changes of the dynamics inside the chaotic windows. Finally, we note that $\bar{T}_2(r)$ in general increases with the parameter a . In fact, its shape is very similar to that of the spectrum of the Lyapunov exponent [6,16]. This reflects the variation of the Lyapunov exponent with a .

Next, we follow Schreiber [10] and study the generalized Baker's map:

$$\begin{aligned} \text{if } v_n \leq \alpha: & \quad u_{n+1} = \beta u_n, \quad v_{n+1} = v_n / \alpha, \\ \text{if } v_n > \alpha: & \quad u_{n+1} = 0.5 + \beta u_n, \\ & \quad v_{n+1} = (v_n - \alpha) / (1 - \alpha). \end{aligned}$$

A time series of length $N=40\,000$ is generated from the map, with nonstationarity introduced through the dependence of $\beta (=n/N)$ with time step n . The dynamics of this system is not as rich as that described by the transient logistic map. However, since the largest Lyapunov exponent of this system does not vary with β ,

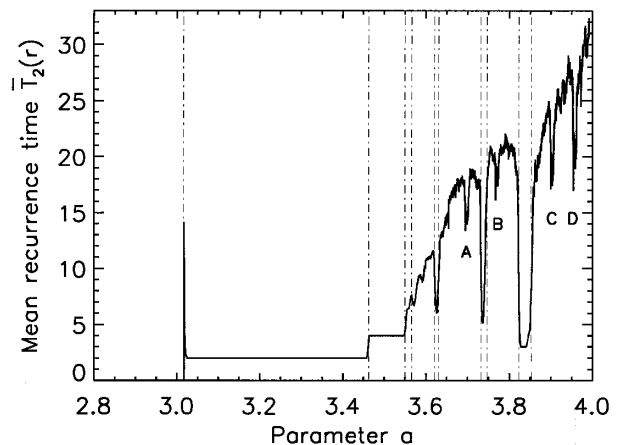


FIG. 4. Variation of $\bar{T}_2(r)$ with the parameter a . Thin dashed-dotted vertical lines are drawn to indicate bifurcations. Capital letters A, B, C, and D are used to indicate the four dips right above them.

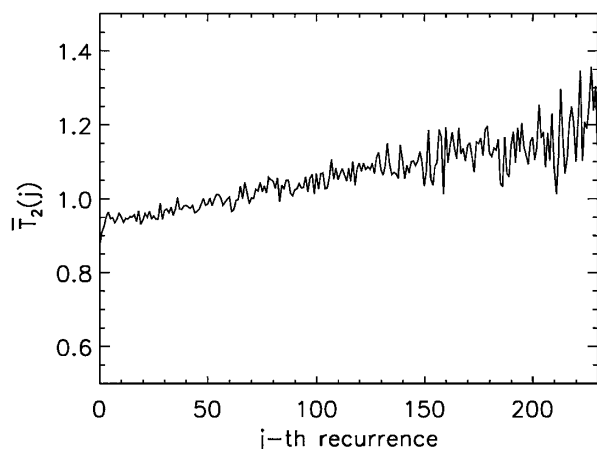


FIG. 5. Variation of $\bar{T}_2(j)$ with j . The scale r used to generate the figure is 2^{-5} . 9000 points are used in the calculation.

this system is somewhat more challenging to a method that aims to detect nonstationarity in a time series. Below, we shall illustrate our second algorithm with this system. Note, however, that the nonstationarity in this system can also be easily detected using our first algorithm.

Following Schreiber [10], we first choose the embedding dimension $m = 2$ and the delay time $L = 1$. We then compute successive recurrence times to $B_r(X_0)$, $T_2(j)$ ($B_r(X_0)$), where j is used to indicate the j th recurrence to $B_r(X_0)$. To eliminate the dependency of $T_2(j)$ on X_0 , we normalize $\{T_2(j)(B_r(X_0)), j = 1, 2, \dots\}$ by its mean, $\bar{T}_2(B_r(X_0))$. This is done for each reference point X_0 . Next we group the normalized $T_2(j)$ together according to j , $\{T_2(j)(X_i), i = 1, 2, \dots\}$, and then compute the mean of each group, $\bar{T}_2(j)$. For nonstationary time series, $\bar{T}_2(j)$ will vary with j , while for stationary time series, $\bar{T}_2(j)$ will have almost a constant value of 1. Figure 5 plots the variation of $\bar{T}_2(j)$ with j , showing that $\bar{T}_2(j)$ almost linearly increases with j . Through sensitivity tests, we find the general trend of this curve does not depend on the particular scale r one uses, as long as r is not too large.

There is a major difference between our methods and the methods of [5–9] in detecting the nonstationarity in a time series. The methods in [5–9] used some statistics from Poincaré recurrence points (sometimes the particular sequence of sojourn points, which starts from the reference point, may be recommended to be removed [9,17]). They may fail to detect the nonstationarity in the following doubly nonstationary process: Successive sojourn times and successive recurrence times are both increasing, and thus keep the density of the Poincaré recurrence points almost constant. A simple realization of such a process would be the following. A person has been traveling between two

cities. He is getting older and slower. Hence his successive sojourn times and recurrence times are both increasing. Yet, during each round trip, on average, he manages to stay a comparable amount of time at each city, and the fraction of time he spends in each city is more or less constant. In contrast, the present method will unambiguously detect the nonstationarity in such a process.

In summary, we have identified two types of recurrence times, and have derived scaling laws relating the mean recurrence times to the information dimension of the attractor. We have also designed two novel ways of using the recurrence time statistics to detect changes in dynamics. These methods may be useful for the analysis of complex time series arising from diverse disciplines of science, such as geophysics, physiology, and finance.

I thank Dr. X.L. Wang of Cambridge University and Professor Paul Rapp of the Medical College of Pennsylvania, Hahnemann University, for arousing and maintaining my interest in this work. I also thank Johnny Lin for English corrections.

-
- [1] M. Kac, *Probability and Related Topics in Physical Sciences* (Interscience, New York, 1959).
 - [2] J.P. Eckmann and D. Ruelle, *Rev. Mod. Phys.* **57**, 617 (1985).
 - [3] V. Balakrishnan, G. Nicolis, and C. Nicolis, *J. Stat. Phys.* **86**, 191 (1997).
 - [4] G.M. Zaslavsky and M.K. Tippet, *Phys. Rev. Lett.* **67**, 3251 (1991).
 - [5] J.P. Eckmann, S.O. Kamphorst, and D. Ruelle, *Europhys. Lett.* **4**, 973 (1987).
 - [6] L.L. Trulla, A. Giuliani, J.P. Zbilut, and C.L. Webber, *Phys. Lett. A* **223**, 255 (1996).
 - [7] R. Manuca and R. Savit, *Physica (Amsterdam)* **99D**, 134 (1996).
 - [8] D.J. Yu, W.P. Lu, and R.G. Harrison, *Phys. Lett. A* **250**, 323 (1998).
 - [9] M.B. Kennel, *Phys. Rev. E* **56**, 316 (1997).
 - [10] T. Schreiber, *Phys. Rev. Lett.* **78**, 843 (1997).
 - [11] J.D. Farmer, E. Ott, and J.A. York, *Physica (Amsterdam)* **7D**, 153 (1983).
 - [12] M. Henon, *Commun. Math. Phys.* **50**, 69 (1976).
 - [13] E.N. Lorenz, *J. Atmos. Sci.* **20**, 130 (1963).
 - [14] P. Grassberger and P. Procaccia, *Phys. Rev. Lett.* **50**, 346 (1983).
 - [15] N.H. Packard, J.P. Crutchfield, J.D. Farmer, and R.S. Shaw, *Phys. Rev. Lett.* **45**, 712 (1980); F. Takens, in *Dynamical Systems and Turbulence*, Lecture Notes in Mathematics Vol. 898, edited by D.A. Rand and L.S. Young (Springer-Verlag, Berlin, 1981), p. 366.
 - [16] A. Wolf, in *Chaos*, edited by A.V. Holden (Princeton University Press, Princeton, NJ, 1986), p. 276.
 - [17] J.B. Gao and Z.M. Zheng, *Phys. Rev. E* **49**, 3807 (1994).